

3-1-2008

Characterization of Zirconium Nitride Films Sputter Deposited with an Extensive Range of Nitrogen Flow Rates

N. Farkas

G. Zhang

R. D. Ramsier

Edward A. Evans

University of Akron Main Campus, evanse@uakron.edu

J. A. Dagata

Please take a moment to share how this work helps you [through this survey](#). Your feedback will be important as we plan further development of our repository.

Follow this and additional works at: http://ideaexchange.uakron.edu/chemengin_ideas

 Part of the [Chemistry Commons](#)

Recommended Citation

Farkas, N.; Zhang, G.; Ramsier, R. D.; Evans, Edward A.; and Dagata, J. A., "Characterization of Zirconium Nitride Films Sputter Deposited with an Extensive Range of Nitrogen Flow Rates" (2008). *Chemical and Biomolecular Engineering Faculty Research*. 12.

http://ideaexchange.uakron.edu/chemengin_ideas/12

This Article is brought to you for free and open access by Chemical and Biomolecular Engineering Department at IdeaExchange@UAkron, the institutional repository of The University of Akron in Akron, Ohio, USA. It has been accepted for inclusion in Chemical and Biomolecular Engineering Faculty Research by an authorized administrator of IdeaExchange@UAkron. For more information, please contact mjon@uakron.edu, uapress@uakron.edu.

Characterization of zirconium nitride films sputter deposited with an extensive range of nitrogen flow rates

N. Farkas

Department of Physics and Department of Chemistry, The University of Akron, Akron, Ohio 44325

G. Zhang

Department of Chemical and Biomolecular Engineering, The University of Akron, Akron, Ohio 44325

R. D. Ramsier

Department of Physics and Department of Chemistry, The University of Akron, Akron, Ohio 44325

E. A. Evans^{a)}

Department of Chemical and Biomolecular Engineering, The University of Akron, Akron, Ohio 44325

J. A. Dagata

Precision Engineering Division, National Institute of Standards and Technology, Gaithersburg, Maryland 20899-8212

(Received 23 May 2007; accepted 9 January 2008; published 20 February 2008)

ZrN_x films are deposited by rf magnetron sputtering using a wide range of nitrogen flow rates to control film properties. Scanned probe microscope (SPM) oxidation is presented as a complimentary characterization tool to x-ray diffraction, colorimetric, and four point probe analyses. The SPM oxidation behavior of the ZrN_x films is related to their structural, optical, and electrical properties. Whereas stoichiometric ZrN films have applications as protective and/or decorative coatings, ZrN_x films sputtered with higher nitrogen flow rates have potential applications in devices where arrays of high aspect ratio nanostructures would be useful. © 2008 American Vacuum Society. [DOI: 10.1116/1.2839856]

I. INTRODUCTION

ZrN_x has been studied extensively for applications in protective and decorative coatings,¹⁻⁴ diffusion barriers,⁵ heat mirrors,⁶ and biomedical⁷⁻⁹ applications; ZrN_x has high wear and corrosion resistance, a high dielectric constant, and reflectivity and is biocompatible.¹⁰ Reactive magnetron sputtering is a widely used method to deposit transition metal nitrides including ZrN_x because of its simplicity, but the properties of the films are highly sensitive to the sputtering conditions.¹¹⁻¹⁴ Several papers have been published concerning systematic studies of the deposition parameters to obtain stoichiometric ZrN with a golden color, high reflectance, and low resistivity.^{1,4,15-17} The appearance of films sputtered with higher nitrogen flow rates is unappealing in the decorative coating industry and consequently these materials are studied less extensively. However, they can be used in other areas besides decorative coatings, where the stoichiometric gold-colored film is not necessarily desired.

In this work, characterization techniques are used to differentiate between the stoichiometric and nonstoichiometric ZrN_x films and we suggest uses for the films with a ratio of Zr:N of less than 1, in particular. The films are prepared using reactive sputtering over a wide range of nitrogen flow rates and then characterized using x-ray diffraction (XRD), four point probe, and colorimetric analyses. Scanned probe microscope (SPM) oxidation is introduced as a characterization technique that is complimentary to the above-mentioned

techniques. We focus our attention on how the kinetics of SPM oxidation are related to the structural, electrical, and optical properties of the ZrN_x films. The results of all characterization methods show consistent transitions in the properties of the films and agree with those described by other researchers. Whereas the stoichiometric ZrN films have applications as protective and/or decorative coatings, the ZrN_x films sputtered with higher nitrogen flow rates have potential applications in devices where arrays of oxide nanostructures with controlled heights less than 200 nm would be useful.

II. EXPERIMENTAL METHODS

A. Film preparation

200 nm thick ZrN_x films were deposited using rf magnetron sputtering of a Zr target in a background of argon and nitrogen; the Zr target has a diameter of 5 cm and a purity of 99.2% (Target Materials, Inc.). Pieces of boron doped (1-3 Ω cm) 500-550 μm thick Si(111) wafers were used as substrates. After ultrasonic cleaning in acetone and then isopropanol for 10 min each, the 1 cm² silicon pieces were placed on a holder positioned 8 cm above the sputtering source. Prior to deposition, the vacuum system was pumped down to 6 × 10⁻⁴ Pa using a turbomolecular pump. The target was sputter cleaned for 20 min in argon [5 SCCM (SCCM denotes cubic centimeter per minute at STP), 55 W] to remove surface oxides and presputtered for 5 min with the same (Ar+N₂) gas mixture used during deposition to stabilize the sputtering conditions. Deposition of the ZrN_x films was performed at a power of 120 W with a constant argon

^{a)}Author to whom correspondence should be addressed; electronic mail: evanse@uakron.edu

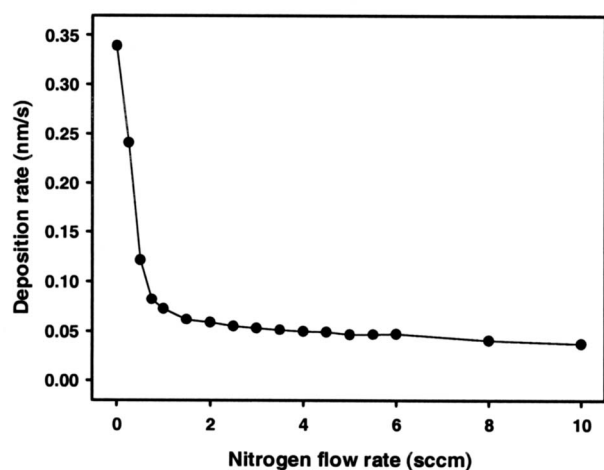


FIG. 1. Deposition rate of ZrN_x films deposited using rf sputtering at an argon flow rate of 2 SCCM, a power of 120 W, and a pressure increasing from 0.3 Pa at the lowest nitrogen flow rate to 0.6 Pa at the highest nitrogen flow rate.

flow rate of 2 SCCM. The nitrogen flow rate was varied from 0 to 10 SCCM in order to change the properties of the ZrN_x thin films. Over this range of flow rates, the system pressure also increased from 0.3 to 0.6 Pa. There was no temperature control and the substrate holder was not biased during deposition.

B. Film characterization

The resulting film thickness and deposition rate were measured with a quartz crystal microbalance. The electrical resistivity and roughness of the films were obtained by four point probe and SPM measurements, respectively. The color of the films was evaluated in the $CIEL^*a^*b$ colorimetric system.¹⁸ A Scintag X-1 x-ray diffractometer was used with $Cu K\alpha$ radiation at a grazing incidence of 0.5° to investigate the crystal structure of the films. The SPM oxidation characterization was performed under ambient conditions at the National Institute for Standards and Technology (NIST) with a TopoMetrix Accurex II operating in contact mode with W_2C -coated silicon cantilevers from Silicon-MDT Ltd.

III. RESULTS AND DISCUSSION

A. Deposition rate

Figure 1 shows the deposition rate as a function of the nitrogen flow rate in the sputtering gas. The deposition rate drops significantly between 0 and 0.75 SCCM nitrogen flow rates followed by a subtle decrease from 1 to 10 SCCM. The sudden decrease in the deposition rate is due to the formation of a nitride layer on the target surface; the sputtering yield of Zr is significantly higher than that of ZrN . The continued decrease in deposition rate for higher nitrogen flow rates is due to the increase in system pressure which lowers the rate of diffusional mass transfer.

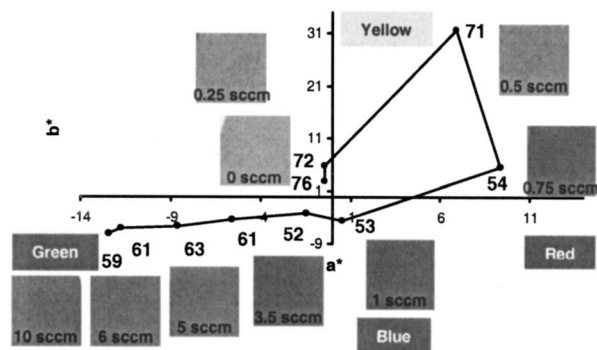


FIG. 2. Color change of the ZrN_x films with respect to the nitrogen content of the sputtering gas in the a^* , b^* plane of the $CIEL^*a^*b$ color space (Ref. 18). The numbers next to data points indicate the relative brightness of the films.

B. Colorimetric properties

It has been reported that the color of transition metal nitride thin films is highly sensitive to the deposition parameters. In the case of ZrN_x , nitrogen flow rate has a strong effect on the color of the film, while the argon can be changed over a fairly wide range without having a significant effect.¹⁵ We fixed the argon flow rate at 2 SCCM and produced film colors of silver, gold, brown, gray, and green by changing the nitrogen flow rate from 0 to 10 SCCM. Figure 2 shows the color change of the ZrN_x films with respect to the nitrogen content of the sputtering gas in the a^* , b^* plane of the $CIEL^*a^*b$ color space.¹⁸ Silver, gold, and golden brown colors are observed as the nitrogen flow rate is increased from 0 to 0.75 SCCM. This dramatic color change occurs in a narrow nitrogen flow rate regime where the deposition rate also drops considerably. The overall color change of the films deposited with a nitrogen flow rate between 0 and 1 SCCM is consistent with the decorative coating literature.^{2,11,15}

As the flow rate of nitrogen is increased further up to 3.5 SCCM, the films turn to a darker gray. Studies concerning colorimetric investigation of ZrN_x films in the higher nitride regime are rare. Dual ion beam sputtered Zr_3N_4 films exhibit a blue color.¹⁹ Here, we report that a green color dominates for films sputtered at 4 SCCM or higher nitrogen flow rates as indicated by the increasingly negative b^* values. The relative brightness of the colors, shown by the numbers located next to the data points, decreases significantly for nitrogen flow rates in the sputtering gas greater than 0.5 SCCM and then slightly increases again for nitrogen flow rates greater than 3.5 SCCM. In this scheme, a brightness value of zero corresponds to black, whereas a value of 100 represents pure white. The color variation of the ZrN_x films is closely related to structural transitions as described below.

C. XRD

Grazing angle XRD analysis reveals structural changes in the films, as shown in Fig. 3. As nitrogen is added to the sputtering plasma, a transition from Zr to ZrN occurs. This

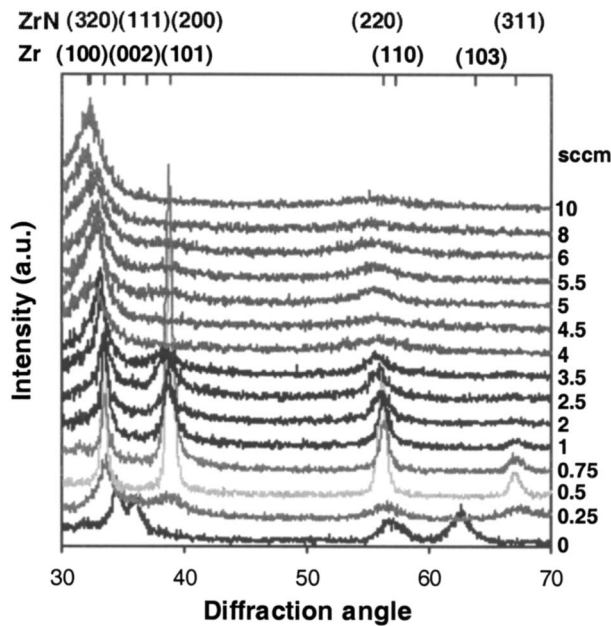


FIG. 3. Grazing angle XRD analysis of ZrN_x films deposited using rf sputtering. Spectra for films deposited with different nitrogen flow rates in the feed (SCCM) are shown. The gold stoichiometric film deposited at 0.5 SCCM nitrogen exhibits dominant $ZrN(200)$ and (111) peaks in the presence of weaker (220) and (311) peaks.

change is also reflected in the color of the films as they turn to yellowish silver. Around 0.5 SCCM, the transition is complete and the gold stoichiometric film exhibits dominant $ZrN(200)$ and (111) peaks in the presence of weaker (220) and (311) peaks. The surface roughness of the golden brown film prepared with 0.75 SCCM is similar to that of the gold-colored film with an even stronger (200) peak.

Films deposited with 1–3.5 SCCM nitrogen flow rates exhibit different XRD patterns. The intensity of the (200) peak drops significantly as the films become gray, while the $ZrN(311)$ peak appears only around the gold-colored regime. With increasing nitrogen content, the color of the films becomes darker gray, and the intensities of the $ZrN(200)$ and (220) peaks continuously decrease. The simultaneous broadening and shifting of the peaks to smaller angles suggest that the films consist of both the polycrystalline ZrN and the progressively forming Zr_3N_4 phase.^{13,20} The transition into the latter occurs as the nitrogen content of the plasma increases above 4 SCCM. The (200) peak disappears and the very broad peak assigned as $Zr_3N_4(320)$ could be explained by the presence of interstitial nitrogen incorporation. Similar trends which eventually lead to the amorphitization of the films and the appearance of the Zr_3N_4 phase have been reported by others.^{13,20}

The effect of nitrogen flow rate on the ratio of the $ZrN(200)$ and (111) peak intensities (I_{200}/I_{111}) and the topography of the films are studied, with the results shown in Fig. 4. We find that the change in the root mean square surface roughness closely follows that of the I_{200}/I_{111} ratio. The (111) planes are close packed planes and are expected to be smoother than the (200) planes. Both graphs have a strong

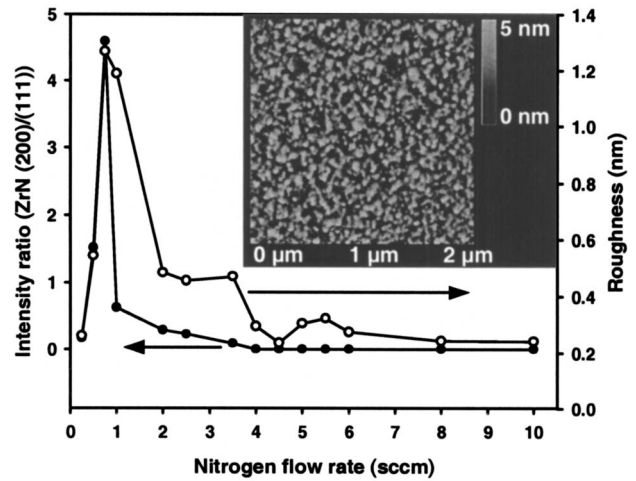


FIG. 4. Plot shows the effect of nitrogen flow rate on the ratio of the $ZrN(200)$ and (111) peak intensities (I_{200}/I_{111}) and the topography of the films (inset). The change in the root mean square surface roughness closely follows that of the I_{200}/I_{111} ratio.

peak at around the stoichiometric flow rate. With increasing nitrogen content of the plasma, both the roughness and the intensity ratios steeply decrease as the films become amorphous. The inset of Fig. 4 presents the surface morphology as imaged by SPM of a ZrN_x film sputtered with 0.75 SCCM nitrogen flow rate.

D. Resistivity

Figure 5(A) shows the variation in electrical resistivity as a function of nitrogen flow rate. The gold-colored films, which are close to stoichiometric ZrN , have low resistivity similar to that of films with a metallic appearance. Then, the resistivity increases gradually through the gray color regime of 1–3.5 SCCM and even more as the nitrogen flow rate reaches the 4 SCCM value. The linearly scaled graph in Fig. 5(B) emphasizes the large resistivity increase at 4 SCCM nitrogen flow rate as the films become amorphous and exhibit a green color.

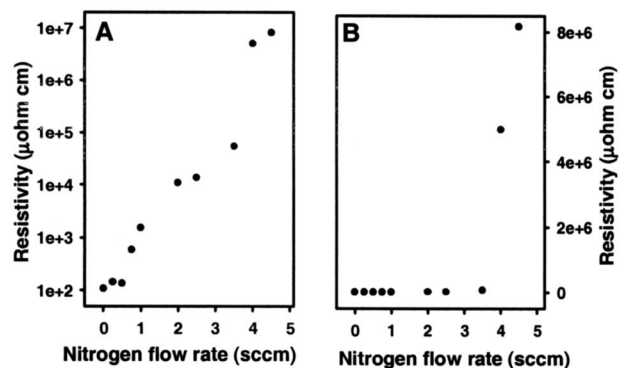


FIG. 5. Plot shows the variation in electrical resistivity as a function of nitrogen flow rate. (A) shows the variation plotted on a semilog plot, while (B) shows the linearly scaled graph.

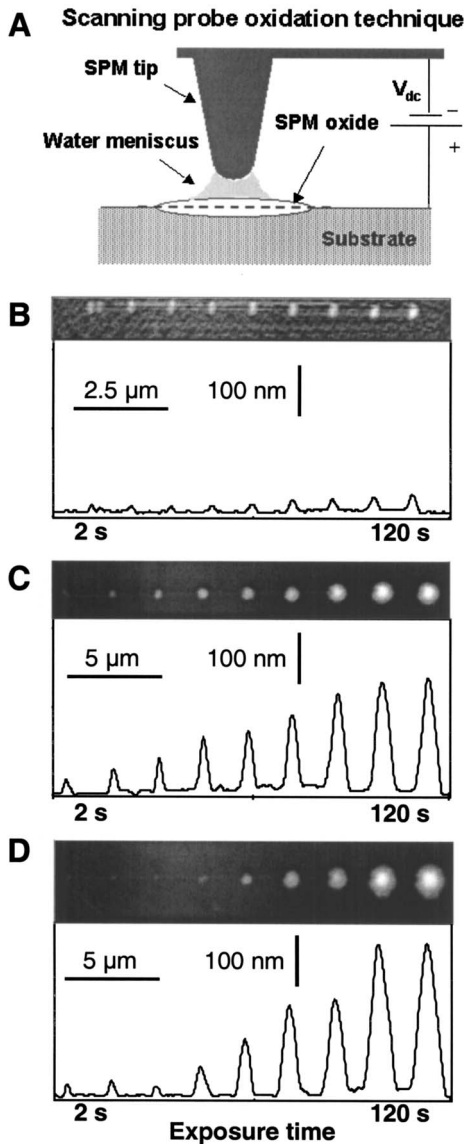


FIG. 6. (A) shows a schematic of the SPM oxidation arrangement used as a new characterization method in this work. Arrays of oxide features are produced as the voltage is applied for a fixed amount of time. The images of the oxide features generated on ZrN_x films with different nitrogen flow rates (0, 3.5, and 5 SCCM, respectively) are acquired in normal contact imaging mode after the oxidation and are shown in (B)–(D).

E. SPM oxidation

Figure 6(A) schematically shows the SPM oxidation arrangement used as a new characterization method in this work. When a sufficiently large negative voltage is applied to the tip with respect to the substrate, almost all materials can be oxidized. Water trapped between the surface and the tip functions as an electrolyte and the high electric field generates oxyanions for the oxide growth. For all the data in this work, the SPM oxidation was performed under ambient conditions in contact mode. The relative humidity was around 30%–35%. Arrays of features are produced as the voltage is applied for a fixed amount of time, then the tip is moved to another location, and the process repeated. The exposure time ranging from 2 to 120 s, applied dc voltage varying

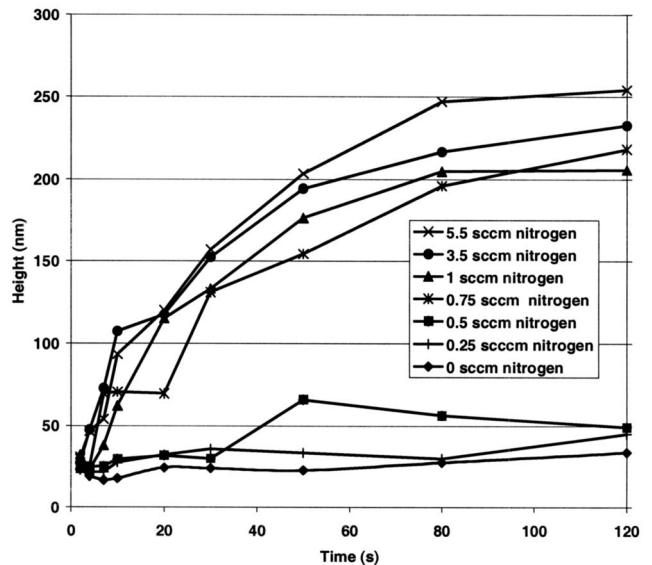


FIG. 7. Representative plots of oxide feature heights plotted as a function of time and nitrogen flow rate at an applied voltage of 30 V. Films deposited with 0.5 SCCM or lower nitrogen flow rate exhibit minimal oxidation, while there is significant oxide growth above this value.

from 10 to 40 V, and tip positioning are all computer controlled. Auger analysis²¹ and secondary ion mass spectrometry verify that oxidation occurs during the process resulting in arrays of oxide features, as seen in the SPM images of Figs. 6(B)–6(D). The images of the oxide features are acquired in normal contact imaging mode after the oxidation. The trend in the height of the features with respect to oxidation time is used to compare films deposited with different nitrogen flow rates in the feed gas; the flow rates of nitrogen used to deposit the films in Figs. 6(B)–6(D) were 0, 3.5, and 5 SCCM, respectively.

SPM oxidation kinetics are sensitive to the film's properties and thus can be used as a characterization tool. Representative SPM images along with matching cross sections of oxide features grown on ZrN_x thin films prepared with different nitrogen flow rates are shown in Figs. 6(B)–6(D). Cross-section analysis of the oxide features allows us to determine their height that can be then plotted as a function of time and nitrogen flow rate. Figure 7 presents a plot with data obtained by applying 30 V for 2–120 s exposure times. Films deposited with 0.5 SCCM or lower nitrogen flow rate exhibit little oxidation, while large features can be grown above this value. It is noticeable that high oxide features are formed on ZrN_x substrates prepared with higher nitrogen flow rates where the deposition rate is low, the resistivity is large, and the films are amorphous.

There is a relationship between the brilliance, resistivity, and the oxidation behavior of the ZrN_x films. This fact facilitates the use of the SPM oxidation technique as a characterization tool. The stoichiometric ZrN films and those prepared with nitrogen flow rate below 0.5 SCCM present high values of brilliance and low resistivity and demonstrate limited SPM oxidation. For films with higher resistivity and lower brilliance, oxide growth is significantly enhanced.

The increases in oxidation rate for the films deposited at the higher nitrogen flow rates can be explained by the subtle changes in the structure of the higher nitrides. The zirconium system is a network former, which means that anions are able to move through channels in the oxide network. As the films obtained with 4 SCCM nitrogen flow rate and above become progressively less crystalline, the capability for the network formation also increases, promoting oxyanion transport and resulting in higher oxide features, as shown in Figs. 6 and 7.

The ZrN_x thin films sputtered with high nitrogen flow rates allow for the reproducible formation of large oxide features with aspect ratios four times greater than features formed on films deposited with low nitrogen flow rates. This SPM oxidation behavior suggests that oxide features with controlled aspect ratio can be made using a parallel writing scheme.²¹ Therefore, applications in which arrays of oxide nanostructures would be useful will benefit from this work. For example, biotemplating requires the modification of surfaces across large areas with well-controlled structures. These structures will facilitate studies of bacterial growth and attachment/alignment of other biological species.

IV. SUMMARY

Optical, structural, electrical, and SPM oxidation characterization studies have been conducted to investigate the effect of nitrogen in the plasma on rf magnetron sputtered ZrN_x thin films. The observed property changes show close relations with one another and divide the films into the following regimes. The understoichiometric and stoichiometric ZrN films exhibit high deposition rate and low resistivity accompanied by minimal SPM oxidation. Films deposited with a 0.5 SCCM nitrogen flow rate have a golden appearance and a polycrystalline ZrN structure.

Nitrogen flow rates between 1 and 3.5 SCCM represent a transition between the stoichiometric and highly overstoichiometric regimes. Based on the broadening and shift of the XRD peaks to smaller angles, the films consist of both polycrystalline ZrN and poorly structured Zr_3N_4 phases. The structural changes are concomitant with increased resistivity and a decrease in the brightness of the gray films. Films deposited with a nitrogen flow rate between 1 and 3.5 SCCM exhibit an enhanced SPM oxide growth. Distinct structural, optical, and electrical transitions have been observed simultaneously at 4 SCCM nitrogen flow rate. Besides the forma-

tion of the amorphous Zr_3N_4 phase, the films become green and their resistivity increases by several orders of magnitude. The SPM oxidation characterization reveals further gradual enhancement of oxide formation.

ACKNOWLEDGMENTS

J.A.D. acknowledges support from Jack Martinez & Steve Knight of the NIST Office of Microelectronics Programs, N.F. acknowledges support from NIST-MEL, and R.D.R. acknowledges support from NIH-NIBIB Grant No. EB003397-01. Acknowledgment is also made to the donors of the American Chemical Society Petroleum Research Fund for partial support of this research.

- ¹S. Niyomsoan, W. Grant, D. L. Olson, and B. Mishra, *Thin Solid Films* **415**, 187 (2002).
- ²E. Budke, J. Krempel-Hesse, H. Maidhof, and H. Schüssler, *Surf. Coat. Technol.* **112**, 108 (1999).
- ³D. Pilloud, A. S. Dehlinger, J. F. Pierson, A. Roman, and L. Pichon, *Surf. Coat. Technol.* **174/175**, 338 (2003).
- ⁴J. V. Ramana, S. Kumar, C. David, A. K. Ray, and V. S. Raju, *Mater. Lett.* **43**, 73 (2000).
- ⁵M. B. Takeyama, T. Itoi, E. Aoyagi, and A. Noya, *Appl. Surf. Sci.* **190**, 450 (2002).
- ⁶K. E. Andersson, M. Veszelei, and A. Roos, *Sol. Energy Mater. Sol. Cells* **32**, 199 (1994).
- ⁷R. Hübler, A. Cozza, T. L. Marcondes, R. B. Souza, and F. F. Fiori, *Surf. Coat. Technol.* **142/144**, 1078 (2001).
- ⁸B. Grössner-Schreiber, M. Griepentrog, I. Hausteine, W.-D. Müller, K.-P. Lange, H. Briedigkeit, and U. B. Göbel, *Clin. Oral Implants Res.* **12**, 543 (2001).
- ⁹J. A. Hendry and R. M. Pilliar, *J. Biomed. Mater. Res.* **58**, 156 (2001).
- ¹⁰K. M. Sherepo and I. A. Red'ko, *Biomed. Eng. (NY)* **38**, 77 (2004).
- ¹¹C.-P. Liu and H.-G. Yang, *Thin Solid Films* **444**, 111 (2003).
- ¹²L. Hu, D. Li, and G. Fang, *Appl. Surf. Sci.* **220**, 367 (2003).
- ¹³H. M. Benia, M. Guemmaz, G. Scherber, A. Mosser, and J.-C. Parlebas, *Appl. Surf. Sci.* **200**, 231 (2002).
- ¹⁴M. Yoshitake, T. Yotsuya, and S. Ogawa, *Jpn. J. Appl. Phys., Part 1* **31**, 4002 (1992).
- ¹⁵M. Nose, M. Zhou, E. Honbo, M. Yokota, and S. Saji, *Surf. Coat. Technol.* **142/144**, 211 (2001).
- ¹⁶R. Hübler, *Surf. Coat. Technol.* **158/159**, 680 (2002).
- ¹⁷H. Yanagisawa, K. Sasaki, Y. Abe, M. Kawamura, and S. Shinkai, *Jpn. J. Appl. Phys., Part 1* **37**, 5714 (1998).
- ¹⁸P. Sullivan, M. Mann, L. Wilburn, and G. DeVries, *Vacuum Technology & Coating*, July, p. 50 (2003).
- ¹⁹S. Camelio, T. Girardeau, L. Pichon, A. Straboni, C. Fayoux, and Ph. Guérin, *J. Opt. A, Pure Appl. Opt.* **2**, 442 (2000).
- ²⁰R. Lamni, E. Martinez, S. G. Springer, R. Sanjinés, P. E. Schmid, and F. Lévy, *Thin Solid Films* **447/448**, 316 (2004).
- ²¹N. Farkas, J. R. Comer, G. Zhang, E. A. Evans, R. D. Ramsier, S. Wight, and J. A. Dagata, *Appl. Phys. Lett.* **85**, 5691 (2004).

Copyright of Journal of Vacuum Science & Technology: Part A is the property of AVS, The Science & Technology Society and its content may not be copied or emailed to multiple sites or posted to a listserv without the copyright holder's express written permission. However, users may print, download, or email articles for individual use.